

Characterization of the 2-Hydroxy-acid Dehydrogenase McyI, Encoded within the Microcystin Biosynthesis Gene Cluster of *Microcystis aeruginosa* PCC7806^{*[5]}

Received for publication, July 24, 2006, and in revised form, October 30, 2006 Published, JBC Papers in Press, December 1, 2006, DOI 10.1074/jbc.M606986200

Leanne A. Pearson, Kevin D. Barrow, and Brett A. Neilan¹

From the School of Biotechnology and Biomolecular Sciences, University of New South Wales, Sydney, New South Wales 2052, Australia

The cyanobacterium *Microcystis aeruginosa* is widely known for its production of the potent hepatotoxin microcystin. This cyclic heptapeptide is synthesized non-ribosomally by the thio-template function of a large modular enzyme complex encoded within the 55-kb microcystin synthetase gene (*mcy*) cluster. The *mcy* gene cluster also encodes several stand-alone enzymes, putatively involved in the tailoring and export of microcystin. This study describes the characterization of the 2-hydroxy-acid dehydrogenase McyI, putatively involved in the production of D-methyl aspartate at position 3 within the microcystin cyclic structure. A combination of bioinformatics, molecular, and biochemical techniques was used to elucidate the structure, function, regulation, and evolution of this unique enzyme. The recombinant McyI enzyme was overexpressed in *Escherichia coli* and enzymatically characterized. The hypothesized native activity of McyI, the interconversion of 3-methyl malate to 3-methyl oxalacetate, was demonstrated using an *in vitro* spectrophotometric assay. The enzyme was also able to reduce α -ketoglutarate to 2-hydroxyglutarate and to catalyze the interconversion of malate and oxalacetate. Although NADP(H) was the preferred cofactor of the McyI-catalyzed reactions, NAD(H) could also be utilized, although rates of catalysis were significantly lower. The combined results of this study suggest that hepatotoxic cyanobacteria such as *M. aeruginosa* PCC7806 are capable of producing methyl aspartate via a novel glutamate mutase-independent pathway, in which McyI plays a pivotal role.

The hepatotoxic microcystins compose the largest and most structurally diverse group of cyanobacterial toxins. Over 65 isoforms of microcystin varying by degree of methylation, hydroxylation, epimerization, peptide sequence, and toxicity have been identified (1). Underlying the extraordinary heterogeneity present among the microcystins is their common cyclic structure and possession of several rare nonproteinogenic amino acid moieties. Collectively, the microcystins may be

described as monocyclic heptapeptides containing both D- and L-amino acids plus N-methyldehydroalanine and a unique β -amino acid side group, 3-amino-9-methoxy-2,6,8-trimethyl-10-phenyldeca-4,6-dienoic acid (Fig. 1) (2). Although various amino acid substitutions can occur within the microcystin cyclic structure, the most common toxin isoform, microcystin LR, contains lysine and arginine at positions 2 and 4, respectively (Fig. 1).

The microcystin biosynthesis (*mcy*) gene cluster was the first complex metabolite gene cluster to be fully sequenced from a cyanobacterium. In *Microcystis aeruginosa* PCC7806, the *mcy* gene cluster spans 55 kb and comprises 10 genes arranged in two divergently transcribed operons, *mcyA–C* and *mcyD–J*. The larger of the two operons, *mcyD–J*, encodes a modular polyketide synthase (McyD), two hybrid enzymes comprising non-ribosomal peptide synthetase (McyE) and polyketide synthase (McyG) modules, and enzymes putatively involved in the tailoring (McyI, McyJ, and McyF) and transport (McyH) of the toxin. The smaller operon, *mcyA–C*, encodes three non-ribosomal peptide synthetases (McyA–C) (3).

Although most open reading frames within the *mcy* gene cluster have been assigned a function based on homologous entries in the data bases, no obvious function could be assigned to the 1014-bp gene *mcyI*. Preliminary sequence analysis of the inferred primary peptide sequence of *mcyI* by Tillett *et al.* (3) revealed a 41% identity to the catalytic region of the *serA*-encoded D-3-phosphoglycerate dehydrogenase (PGDH²; EC 1.1.1.95) from *Methanobacterium thermoautotrophicum* (4). Although this archaeal PGDH homolog has not yet been characterized, extensive research has been carried out on PGDH homologs from other organisms, including mammals, plants, and bacteria.

PGDH belongs to the 2-hydroxy acid family of dehydrogenases and catalyzes the first committed step in the phosphorylated serine biosynthesis pathway: the oxidation of 3-phosphoglycerate (3-PGA) to 3-phosphohydroxypyruvate, with the concomitant reduction of NAD to NADH. Interestingly, PGDH is also capable of catalyzing the interconversion of α -ketoglutarate

^{*} This work was supported by the Australian Research Council and the Cooperative Research Centre for Water Quality and Treatment. The costs of publication of this article were defrayed in part by the payment of page charges. This article must therefore be hereby marked "advertisement" in accordance with 18 U.S.C. Section 1734 solely to indicate this fact.

[5] The on-line version of this article (available at <http://www.jbc.org>) contains supplemental Fig. S1.

¹ To whom correspondence should be addressed. Tel.: 612-9385-3235; Fax: 612-9385-1591; E-mail: b.neilan@unsw.edu.au.

² The abbreviations used are: PGDH, D-3-phosphoglycerate dehydrogenase; 3-PGA, 3-phosphoglycerate; α -KG, α -ketoglutarate; 2-HGA, 2-hydroxyglutarate; LDH, D-lactate dehydrogenase; MDH, malate dehydrogenase; Mal, malate; OAA, oxalacetate; MeAsp, methyl aspartate; 3-MeMal, 3-methyl malate; MES, 4-morpholineethanesulfonic acid; 3-MeOAA, 3-methyl oxalacetate; ACT, aspartokinase chorismate mutase and TyrA (prephenate dehydrogenase).

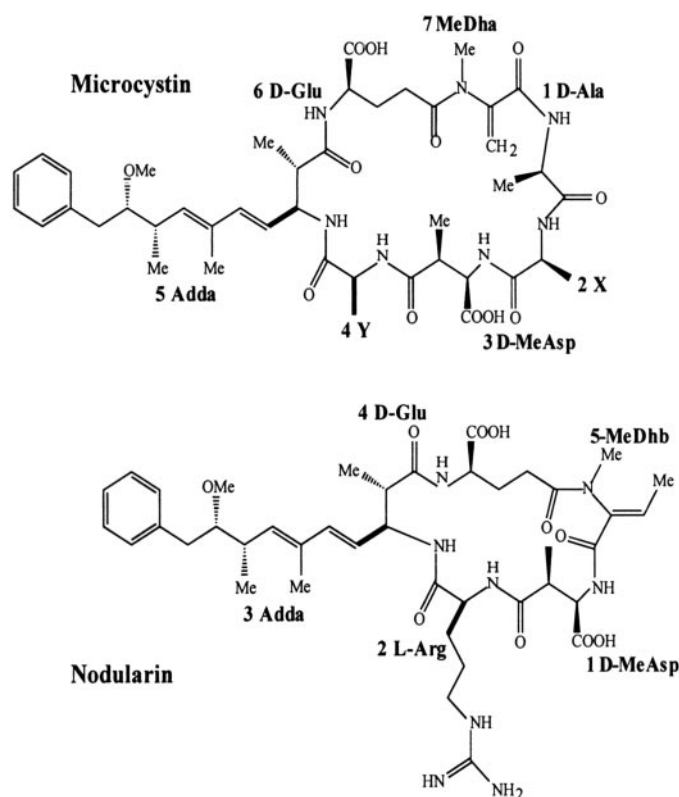


FIGURE 1. Structure of the cyanobacterial hepatotoxins microcystin and nodularin. The general numbering of residues is indicated. The two variable amino acids in microcystin are indicated by X and Y. The most common isoform is microcystin LR, where X is L-Leu and Y is L-Arg. MeDha, N-methyldehydroalanine; Adda, 3-amino-9-methoxy-2,6,8-trimethyl-10-phenyldeca-4,6-dienoic acid; MeDhb, methyldehydrobutyryne.

arate (α -KG) and 2-hydroxyglutarate (2-HGA) (5). The D-2-hydroxy-acid dehydrogenase family also includes D-lactate dehydrogenase (LDH; EC 1.1.1.28) and malate dehydrogenase (MDH; EC 1.1.1.37), which catalyze the conversion of lactate to pyruvate and malate (Mal) to oxalacetate (OAA), respectively. The family members share an overall sequence identity of ~22% and a similarity of ~50% (6). These enzymes also possess a conserved nucleotide-binding motif that preferentially binds to either NAD(H) or NADP(H).

Despite its similarity to PGDH and other 2-hydroxy-acid dehydrogenases, McyI was originally predicted to function as a dehydratase enzyme, playing a role in microcystin biosynthesis by catalyzing the dehydration of serine to dehydroalanine (3). The recently sequenced nodularin gene cluster of *Nodularia spumigena* NSOR10 also encodes a 2-hydroxy-acid dehydrogenase homolog, NdaH. Like McyI, this enzyme was originally predicted to catalyze a dehydration reaction: the conversion of threonine to dehydrobutyryne (7). Although the microcystin and nodularin biosynthesis pathways may involve serine/threonine dehydration reactions, it is unlikely that these reactions are catalyzed by McyI and NdaH, as originally predicted. McyI and NdaH are homologous to 2-hydroxy-acid dehydrogenases, and this family of enzymes is neither structurally nor functionally related to the family of dehydratase enzymes known to convert serine to dehydroalanine in other secondary metabolite pathways (8). Whereas dehydrogenases such as PGDH catalyze redox reactions (*i.e.* the transfer of elec-

trons involving pyridinium nucleotides), the amino-acid dehydratases catalyze dehydration and rehydration reactions (*i.e.* the removal or addition of H_2O). The chemical nature of these reactions and their respective substrates are very different. Therefore, alternative putative functions for McyI and NdaH in hepatotoxin production needed to be investigated.

As McyI shares sequence homology with PGDH, the first committed step in the phosphorylated serine biosynthesis pathway, it is conceivable that this enzyme may also play a role in serine metabolism. However, as no other serine biosynthesis enzymes (*e.g.* phosphoserine transaminase and phosphoserine phosphatase) are encoded within the *mcy* gene cluster, it is unlikely that McyI is involved in the production of this non-polar amino acid.

An alternative hypothesis is that McyI is involved in the production of the methyl aspartate unit (MeAsp³) of the microcystin cyclic structure. A feeding study with [1,2-¹³C]acetate suggested that the MeAsp residues in microcystin and nodularin are synthesized via a condensation reaction between acetyl-CoA and pyruvic acid. 2-Hydroxy-2-methylsuccinic acid is then converted to 2-hydroxy-3-methylsuccinic acid, oxidized to 2-oxo-3-methylsuccinic acid, and finally transaminated to MeAsp (9). As McyI is a 2-hydroxy-acid dehydrogenase homolog, we predict that this enzyme catalyzes the interconversion of 2-hydroxy-3-methylsuccinic acid (3-methyl malate) to 2-oxo-3-methylsuccinic acid (3-methyl oxalacetate), the penultimate step in methyl aspartate biosynthesis (Fig. 2).

This study describes the bioinformatics, genetic, and enzymatic characterization of McyI. The results of these experiments are discussed with respect to the role of this unique methyl-malate dehydrogenase in microcystin biosynthesis.

EXPERIMENTAL PROCEDURES

Cyanobacterial Strains and Cultures—The microcystin-producing strain *M. aeruginosa* PCC7806 was kindly provided by E. Dittmann (Institute for Biology, Humboldt University, Berlin). Other cyanobacteria were obtained from the Institute for Biology, the Microbiology Division of the Biocenter at the University of Helsinki (Helsinki, Finland), and the cyanobacterial culture collection (University of New South Wales).

Cyanobacteria were grown as batch cultures in BG11 medium (Fluka) under 16 μ mol photons $m^{-2} s^{-1}$ white light. Light intensities were measured using a LI-COR LI-250 light meter (LI-COR Biosciences). The absorbance (A_{680}) of the cultures was measured using an Ultrospec II spectrophotometer (Biochrom Ltd.).

Cyanobacterial DNA Extractions—DNA was isolated from cyanobacteria according to the xanthogenate-SDS method of Tillett and Neilan (10).

Screening Various Strains of Cyanobacteria for *mcyI* Orthologs—The degenerate oligonucleotide primers *mcyI*degenF (5'-TGTGCGTTATCCTAMTAA-3') and *mcyI*degenR (5'-GGCTTCTCDCCCTGAAGC-3') were designed to amplify, via PCR, an ~790-bp sequence within the *mcyI* locus of *M. aeruginosa* PCC7806 and *Anabaena* sp. 90. These primers were used to screen chromosomal DNA samples from several toxic and nontoxic strains of cyanobacteria for *mcyI* orthologs (see Table 1).

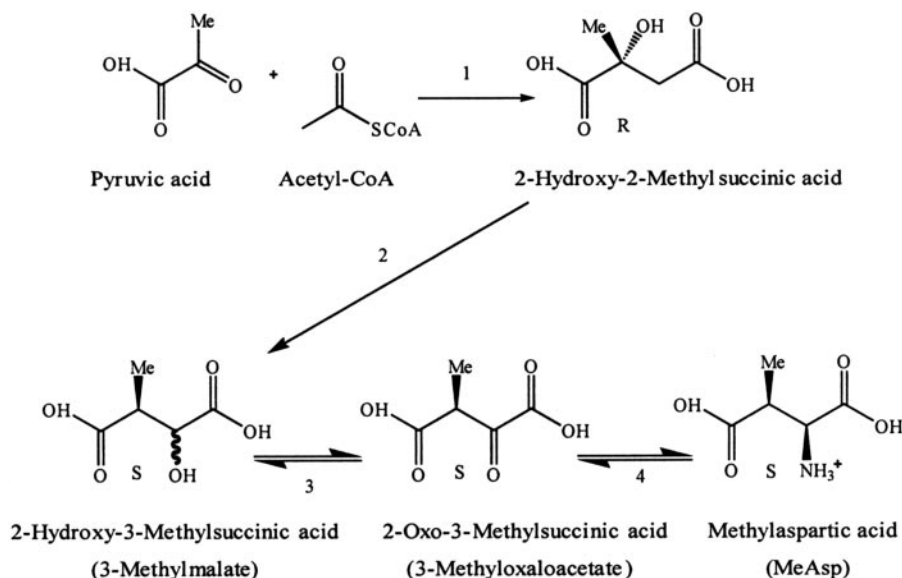


FIGURE 2. Putative reaction pathway to MeAsp in microcystin and nodularin biosynthesis. Adapted from Moore (Ref. 37). Step 3 is putatively catalyzed by *McyI* (or *NdaH* in the case of nodularin production).

Sequence Analysis—The 1011-bp DNA sequence of *mcyl* (complement of nucleotides 2004–3017; GenBank™ accession number AF183408) was analyzed using several different computer programs accessed via the ExPASy proteomics server. Codon usage within the *mcyl* sequence was assessed with the Countcodon program (Kazusa DNA Research Institute). The percentage similarity and identity scores of *McyI* and other peptide sequences were determined using the PSI-BLAST program (NCBI). Conserved domains within *McyI* were detected using CD-Search (NCBI) and ScanProsite (ExPASy).

Phylogenetic Analysis—A PSI-BLAST search with the *McyI* sequence returned 26 sequences with BLAST scores >200 (see Table 2). These sequences were subsequently used to generate a multiple sequence alignment and corresponding phylogenetic tree (ClustalX). Four reference sequences from characterized enzymes (PGDH, LDH, MDH, and formate dehydrogenase) were also included, as was *Escherichia coli* NAD-independent D-lactate dehydrogenase. The latter was designated as an artificial outgroup because it is a membrane-bound FAD flavoenzyme and does not belong to the D-isomer-specific 2-hydroxyacid dehydrogenase family (11). Phylogenetic trees were generated using the neighbor-joining method with gaps removed. Trees were displayed graphically using NJplot and AppleWorks Version 6 (Apple Computer, Inc.).

Overexpression of Histidine-tagged *McyI*—Expression cultures were inoculated with 1% overnight starter culture (Rosetta(DE3)pLysS plus pET30(*mcyl*)) and grown in Tryptone phosphate medium supplemented with kanamycin (50 μ g/ml) and chloramphenicol (34 μ g/ml). Cultures were grown with vigorous shaking (160 rpm) at 37 °C to $A_{650} = 0.6$ and either retained at 37 °C or transferred to 30 or 25 °C and incubated for an additional 20 min (or until $A_{650} \sim 1.0$). Expression of *McyI* was subsequently induced with 1 mM isopropyl β -D-thiogalactopyranoside for 0–18 h at 25–37 °C. Cell pellets were harvested by centrifugation $5000 \times g$ for 10 min at 4 °C, washed

with phosphate buffer (0.5 M NaCl and 20 mM sodium phosphate (pH 7.4)), and stored at -80 °C until required.

Purification of Histidine-tagged *McyI*—Cell pellets were thawed on ice, resuspended in 2% of the original culture volume of cold phosphate buffer containing 1 mM phenylmethylsulfonyl fluoride, passed several times through an 18-gauge needle, and then briefly sonicated (Branson Sonifier model 250; amplitude of 25, 50% duty cycle, pulsed). The lysate was cleared by centrifugation at $20,000 \times g$ for 30 min at 4 °C and precipitated on ice using 40% ammonium sulfate. The final pellet was resuspended in 0.4% of the original culture volume of cold phosphate buffer containing 100 mM imidazole, filtered through a

22- μ m membrane, and applied to a 5-ml HiTrap column (Amersham Biosciences) charged with Ni^{2+} . The column was washed with 10 column volumes of phosphate buffer containing 100 mM imidazole and eluted with 2 column volumes of phosphate buffer containing 300 mM imidazole. The wash and eluate were collected in 1-ml volumes and analyzed by SDS-PAGE (12% polyacrylamide gels) and Western blotting using a nickel-nitrilotriacetic acid-alkaline phosphatase conjugate (Qiagen Inc.) with 5-bromo-4-chloro-3-indolyl phosphate/nitro blue tetrazolium staining (Sigma). Purified protein samples intended for enzyme assays were desalted by size exclusion filtration using Amicon Ultra 10-kDa cutoff columns and 50 mM HEPES exchange buffer (pH 7).

Determining the Subunit Organization of Native *McyI*—The molecular masses of the individual subunits of *McyI* were estimated by size exclusion chromatography using an ÄKTA Basic 900 series fast protein liquid chromatography apparatus fitted with a Frac-920 fraction collector, a UV detector, and a Superdex 200 10/300 GL column (Amersham Biosciences). The column was equilibrated with wash buffer (50 mM sodium phosphate (pH 7) and 150 mM NaCl) and calibrated with ~ 1 mg each of seven molecular mass standards (Sigma) (see Fig. 6). One milligram of purified *McyI* was subsequently loaded. All samples were run at a flow rate of 0.5 ml/min. Eluted proteins were detected spectrophotometrically (220–280 nm) and collected in 250- μ l fractions. Standard curves (log of subunit molecular mass versus volume eluted) were based on the molecular masses of the protein standards. The eluted *McyI* fractions were diluted to 5 μ g/ml and checked for activity by performing an OAA reductase assay (see below).

Chemical Synthesis of 2-Hydroxy-3-methylsuccinic Acid—2-Hydroxy-3-methylsuccinic acid (3-methyl malate (3-Me-Mal)) was synthesized by reduction of diethyl oxalpropionate (10 g, 0.05 mol; Aldrich) in 95% ethanol (100 ml) by the addition of an 8-fold excess of sodium borohydride (3.8 g, 0.1 mol). After the mixture was stirred at room temperature for 24 h, 4 M HCl

Characterization of McyI

(20 ml) was slowly added, and the most of the ethanol evaporated under reduced pressure. Saturated sodium chloride solution (100 ml) was added, and the mixture was extracted five times with ethyl acetate (100 ml). The combined extracts were filtered, dried (MgSO_4), and evaporated, yielding a viscous oil (4.5 g, ~45%). The ^1H NMR spectrum (CDCl_3) showed signals for the *threo*-isomer (δ 1.07 (d, J = 7.2 Hz, 3-Me) and 2.9 (m, H-3)) and the *erythro*-isomer (δ 3.0 (m, H-3)). The ratio of the *threo*- to *erythro*-isomers was 1:6. The other signals of the two isomers (*erythro* and *threo* H-2 and *erythro* 3-Me signals) are underneath the CH_2 resonances (δ 4.1–4.3) and the CH_3 resonances (δ 1.1–1.2) of the ethyl ester groups (data not shown).

Hydrolysis of the crude esters (2.0 g) was carried out by refluxing with 4 M HCl (50 ml) for 4 h. The cooled mixture was diluted with water (100 ml) and extracted with ethyl acetate (2×50 ml) to remove any unhydrolyzed esters and some unsaturated acids formed. The aqueous phase was evaporated to dryness, giving an oil (1.2 g). This was left to stand at -20°C for 72 h after approximately half had crystallized. The oily crystals were washed briefly with cold chloroform, in which hydroxymethylsuccinic acids are insoluble, leaving a colorless crystalline solid (0.54 g). The 600-MHz ^1H NMR ($^2\text{H}_2\text{O}$) spectrum now showed only the clearly resolved resonances for the two isomers (*threo/erythro* ratio of 1:6): *threo*-isomer, δ 4.54 (d, J = 4.05 Hz, H-2), 2.91 (m, H-3), and 1.0 (d, J = 7.14 Hz, 3-Me); and *erythro*-isomer, δ 4.28 (d, J = 4.17 Hz, H-2), 2.97 (m, H-3), and 1.05 (d, J = 7.20 Hz, 3-Me). The latter assignments are identical to those reported for the *erythro*-isomer (12). The resonances are also consistent with earlier NMR data recorded at lower fields and thus lacking some of the dispersion reported here for both the free acids and some derivatives (13–15). No attempts were made to separate these two isomers, and they were used as inhibitors in the ratio indicated above.

Oxidoreductase Assays—The dehydrogenase and reductase activities of recombinant McyI were analyzed in triplicate in 1-ml cuvettes. The production or disappearance of NAD(P)/H was monitored spectrophotometrically at 340 nm using a Cary 100 UV spectrophotometer (Varian, Inc.). Reactions were initiated by the addition of substrate or enzyme.

The dehydrogenase activities of McyI were measured by monitoring the conversion of NADP to NADPH. Each reaction contained 1 mM NADP, 0.1–10 mM substrate (3-MeMal, D-Mal, L-Mal, D-2-HGA, D-3-PGA), and 50 μg of purified McyI in 1 ml of assay buffer. The production of NADPH was monitored spectrophotometrically at 340 nm for 0.5–1 min at 37°C .

The reductase activities of McyI were measured by monitoring the conversion of NADPH to NADP. Each reaction contained 0.25 mM NADPH, 0.1–5 mM substrate (α -KG or OAA), and 2–5 μg of purified McyI in 1 ml of assay buffer. The disappearance of NADPH was monitored spectrophotometrically at 340 nm for 0.5–1 min at 37°C .

End Product Analysis—The end products of the Mal/OAA oxidoreductase reactions were analyzed by NMR spectroscopy. NMR spectroscopy was carried out on a Bruker Advance DMX-600 spectrometer using a triple broadband inverse probe. ^1H NMR spectra were acquired at 600.13 MHz with a 90° pulse of 9 μs , a spectral width of 8992 Hz, 33,000 data points and a 2-s delay between pulses. Samples were run in 0.5 ml of 95% potas-

sium phosphate (pH 7) and 5% $^2\text{H}_2\text{O}$. The standard Bruker water saturation pulse program was used. The free induction decay was zero-filled to 64,000 data points and processed with a line-broadening factor of 1 Hz before Fourier transformation.

Determining the Optimal pH of the McyI OAA Reductase Assay—The pH optimum for the McyI OAA reductase assay was determined by monitoring the disappearance of NADPH at 340 nm over a pH range of 5.5–9 at 25°C . Each 1-ml reaction contained 0.25 mM NADPH, 0.8 mM OAA, and 5 μg of purified McyI in 1 ml of assay buffer (1.0 mM dithiothreitol, 0.1 mM phenylmethylsulfonyl fluoride, and 100 mM buffer (MES at pH 5.5–6.5, HEPES at pH 7–8, or Tris-Cl at pH 8.5–9)).

Determining the Optimal Temperature and Thermostability of the McyI OAA Reductase Assay—The temperature optimum for the McyI OAA reductase assay was determined by monitoring the disappearance of NADPH at 340 nm over a temperature range of 25 – 60°C . Each 1-ml reaction contained 0.25 mM NADPH, 0.8 mM OAA, and 5 μg of purified McyI in 1 ml of assay buffer (pH 7). The stability of McyI at different temperatures was determined by incubating the enzyme for 3 min at 25 – 60°C and then chilling it immediately on ice prior to performing the OAA reductase assay at 37°C as described above.

McyI Specificity—Various structurally related compounds (lactate, pyruvate, D-Ser, L-Ser, L-Phe, oxalic acid, cinnamate, phenyl acetate, phenyl lactate, phenylalanine, and diethyl oxalpropionate; 0.1–10 mM) were tested as substrates of McyI in the forward (dehydrogenase) or reverse (reductase) direction at 37°C for 1 min at pH 7 as described above. To test whether McyI is able to use non-phosphorylated cofactors, the 3-MeMal, Mal, OAA, and α -KG oxidoreductase assays were repeated using NAD/H in place of NADP/H.

McyI Kinetic Analysis—Kinetic analysis of the α -KG and OAA reductase activities of McyI was carried out in 1-ml reactions each containing 0.25 mM NADPH, 5 μg of purified enzyme, and various amounts of substrate in reaction buffer (pH 7). Initial velocities were measured by monitoring the disappearance of NADPH at 340 nm for 0.5 min at 37°C .

Kinetic analysis of the NADPH oxidase activity of McyI was performed in 1-ml reactions each containing 5 μg of purified enzyme, 0.8 mM OAA, and various amounts of NADPH in reaction buffer (pH 7). Initial velocities were measured as described above.

Inhibition Assays—The inhibitory effects of various substances on the OAA and α -KG reductase activities of McyI were tested. Assays were performed in 1 ml of reaction buffer (pH 7) containing 0–100 mM putative inhibitor (L-Ser, 3-MeMal, L-Mal, D-Mal, L-Asp, D-Asp, D-2-HGA, or D-3-PGA), 0.25 mM NADPH, 5 μg of enzyme, and 0.2 mM OAA or 1 mM α -KG. The disappearance of NADPH was monitored spectrophotometrically at 340 nm for 0.5–1 min at 37°C .

RESULTS

Distribution of *mcyl* Orthologs in Various Species of Cyanobacteria—To assess the distribution of *mcyl* orthologs among toxic and nontoxic cyanobacteria, DNAs from 24 different strains were screened by PCR with degenerate oligonucleotide primers. The results are presented in Table 1. All microcystin-producing strains, except for *Planktothrix agardhii*

TABLE 1

Distribution of *mcyl* orthologs among toxic and nontoxic cyanobacteria

Strain	Ref./source	Microcystin ^a	<i>mcyl</i> degenF/R ^b
<i>Anabaena cylindrica</i> PCC7122	Ref. 38	—	—
<i>Anabaena flosaquae</i>	UTEX ^c	—	—
<i>Anabaena</i> PCC7108	Ref. 39	—	+
<i>Anabaena</i> sp. 90	Ref. 40	+	+
<i>M. aeruginosa</i> HUB 5.3	Ref. 41	—	+
<i>M. aeruginosa</i> NIES298	NIES ^c	+	+
<i>M. aeruginosa</i> PCC7005	PCC ^c	+	+
<i>M. aeruginosa</i> PCC7804	PCC	+	+
<i>M. aeruginosa</i> PCC7806	Ref. 42	+	+
<i>M. aeruginosa</i> PCC7820	Ref. 42	+	+
<i>M. aeruginosa</i> UWOC MR-A	Ref. 43	+	+
<i>M. aeruginosa</i> UWOC MR-C	Ref. 43	—	+
<i>M. aeruginosa</i> UWOC MR-D	Ref. 43	+	+
<i>M. aeruginosa</i> UWOC CBS	Ref. 44	—	+
<i>M. aeruginosa</i> UWOC E7.GC	Ref. 44	+	+
<i>Microcystis viridis</i> NIES102	Ref. 45	+	+
<i>Microcystis wesenbergii</i> NIES107	NIES	+	+
<i>Microcystis</i> PCC7840	PCC	+	+
<i>Microcystis</i> sp. UTEX2664	UTEX	+	+
<i>Microcystis</i> ssp. UTEX2667	UTEX	+	+
<i>Nodularia harveyana</i> PCC73104	PCC	N ^c	—
<i>N. spumigena</i> NSOR10	Ref. 46	N	—
<i>P. agardhii</i> CYA126	Ref. 22	+	—
<i>Synechocystis</i> PCC6803	PCC	—	—

^a Production of toxins was detected by mouse bioassay, high pressure liquid chromatography, or enzyme-linked immunosorbent assay.

^b *mcyl* orthologs were detected by PCR using *mcyl*degenF/R.

^c UTEX, University of Texas; NIES, National Institute for Environmental Studies; PCC, Pasteur Culture Collection; N, nodularin-producing strain.

CYA126, tested positive for *mcyl*. However, *mcyl* orthologs were not detected in the nodularin-producing strains. Interestingly, nearly half of all the nontoxic cyanobacteria screened also tested positive for *mcyl*.

Sequence Analysis of *mcyl*—The 1014-bp *mcyl* open reading frame was predicted to encode a 36.71-kDa peptide with a pI of 5.62. Although dense alignment surface (DAS) method analysis indicated two possible membrane-spanning domains within Mcyl (between residues 123 and 125 and residues 163 and 164), these were in the low confidence range. The Kyte-Doolittle plot (ProtScale) suggested that the Mcyl peptide is largely hydrophilic, although several small hydrophobic regions were identified (data not shown).

PSORTb gave a cytoplasmic localization score of 9.26, indicating that Mcyl is a cytoplasmic protein. The *mcyl* sequence contains 32 rare codons, including several repeated and/or consecutive rare codons. Subsequent heterologous expression studies were therefore carried out in the Rosetta(DE3)pLysS expression strain containing the pRARE plasmid encoding these rare *E. coli* tRNA codons.

Comparison of the inferred primary peptide sequence of *mcyl* with other sequences in the NCBI Database revealed significant similarity (up to 72% identity and 84% similarity using PSI-BLAST) to putative and experimentally characterized enzymes, mainly PGDHs, of bacterial (mostly cyanobacterial), archaeal, and eukaryotic origins. The top five PSI-BLAST results were sequences from *N. spumigena* (71% identity and 84% similarity), *Anabaena* sp. (72% identity and 84% similarity), *Methanopyrus kandleri* (43% identity and 64% similarity), *Rubrobacter xylanophilus* (42% identity and 60% similarity), and *Methanothermobacter thermautotrophicus* (41% identity and 61% similarity) (see Table 2 for accession numbers). A genomic BLAST search was also performed to

identify previously characterized *E. coli* homologs. The returned sequences included 2-keto-D-gluconate reductase, PGDH, LDH, and erythronate-4-phosphate dehydrogenase, although scores were generally quite low ($\leq 32\%$ identity and 50% similarity). BL2SEQ analysis was also performed for Mcyl and *E. coli* PGDH (NCBI accession number P08328) and returned scores of 31% identity and 48% similarity. The individual domains of Mcyl (putative nucleotide and substrate domains) were also analyzed by blastp; however, the results generally reflected those of the full-length blastp search, *i.e.* no new sequences were returned.

A ScanProsite pattern search also identified D-isomer-specific 2-hydroxy-acid dehydrogenase NAD-binding signatures (LIVMA)(AG)(IVT)(LIVMFY)(AG)XG(NHKRQGSAC)(LIV)GX_{13,14}(LIVMFT)X₂(FYWCTH)(DNSTK) at residues 158–186 of the Mcyl peptide (Fig. 3). Enzymes possessing these signatures are structurally related and have similar enzyme activities (16–18).

The sequence alignment of Mcyl with other cyanobacterial homologs and *E. coli* PGDH revealed that Mcyl from *M. aeruginosa* and *Anabaena* sp. and NdaH (*N. spumigena*) lack ~72 amino acids that compose the corresponding C-terminal regulatory (ACT) domain, making them, on average, 18% shorter than *E. coli* PGDH. Several other sequence variations between Mcyl and PGDH were also apparent (Fig. 3).

To gain an overview as to the relative phylogenetic position of Mcyl within the 2-hydroxy-acid dehydrogenase family, a phylogenetic analysis was performed. Sequence lengths used in the analysis ranged from 306 to 624 amino acids (Table 2). The phylogenetic tree (Fig. 4) partitioned into three main subgroups. Subgroup A, which contains Mcyl, is composed exclusively of sequences from the hepatotoxin biosynthesis gene clusters of cyanobacteria. Subgroup B is composed of putative dehydrogenases from *Arabidopsis thaliana*, several species of cyanobacteria, and the thermophilic actinobacterium *R. xylanophilus*. Subgroup C consists mostly of archaeal proteins, with the exception of two eubacterial sequences, *Thermoanaerobacter tengcongensis* (order Clostridiales) and *Oceanobacillus ihelyensis* (order Bacillales).

Approximately one-third of all sequences in the phylogenetic tree possess amino acid C-terminal regulatory domains. Although these regulatory domains are present in each organismic lineage, they are most prevalent in the plant and archaeal subgroups. Clustering of ACT domain-possessing proteins within each organismic lineage is apparent.

The tree also demonstrates that subgroups B and C share a common ancestor that had an earlier divergence leading to the subgroup A lineage of cyanobacterial proteins. The distribution of the reference sequences within the tree supports the prediction that the subgroup A/B/C lineage evolved from a common PGDH ancestor rather than the ancestral MDH, LDH, or formate dehydrogenase.

Overexpression and Purification of Histidine-tagged Mcyl—Mcyl was overexpressed in *E. coli* with an N-terminal hexahistidine fusion tag. The recombinant peptide was highly expressed under all culture/induction conditions tested. Western blot analysis confirmed that Mcyl was expressed without truncation at the expected molecular mass of ~40 kDa. Maxi-

TABLE 2

Sequences used to create the phylogenetic tree in Fig. 4

Organism	Protein	Primary function ^a	Length ^b	Accession no. ^c
<i>Anabaena</i> sp.	McyI		337	AA062580
<i>A. thaliana</i>			602	NP_195146
<i>A. thaliana</i>	PGDH	D-3-Phosphoglycerate dehydrogenase	624	T52296
<i>A. thaliana</i>	PGDH	D-3-Phosphoglycerate dehydrogenase	603	AAM60833
<i>Archaeoglobus fulgidus</i>			527	NP_069647
<i>Crocospaera watsonii</i>			525	ZP_00179809
<i>E. coli</i>	LDH (LdhA)	Fermentative D-lactate dehydrogenase	329	AAB51772
<i>E. coli</i>	PGDH (SerA)	D-3-Phosphoglycerate dehydrogenase	410	P08328
<i>E. coli</i>	DLD	D-Lactate dehydrogenase (NADH-independent)	571	AAC75194
<i>Flaveria trinervia</i>	MDH	D-Malate dehydrogenase	385	AAA87008
<i>Methanocaldococcus jannaschii</i>			524	NP_248012
<i>M. kandleri</i>			522	NP_613584
<i>Methanothermobacter thermoautotrophicus</i>			525	NP_276105
<i>M. aeruginosa</i>	McyI		337	AAF00955
<i>M. aeruginosa</i>	McyI		337	AB032549
<i>N. spumigena</i>	NdaH		341	AA064409
<i>Nostoc punctiforme</i>			526	ZP_00112058
<i>Nostoc</i> sp.			526	NP_485930
<i>O. iheyensis</i>			319	NP_693766
<i>Pseudomonas</i> sp.	FDH	NAD-dependent formate dehydrogenase	401	P33160
<i>Pyrococcus abyssi</i>			307	NP_126444
<i>Pyrococcus furiosus</i>			306	NP_579123
<i>R. xylanophilus</i>			527	ZP_00199880
<i>Synechococcus elongatus</i>			529	ZP_00164567
<i>Synechocystis</i> sp.			554	NP_441198
<i>Synechocystis</i> sp.			528	NP_896628
<i>T. tengcongensis</i>			533	NP_624129
<i>Thermosynechococcus elongatus</i>			527	NP_681115
<i>Trichodesmium erythraeum</i>			527	ZP_00327083

^a Primary enzymatic function is given for experimentally characterized proteins only.

^b The values indicate the lengths of the amino acid sequences.

^c These are the NCBI accession numbers. References can be found in the corresponding data base files.

mal yields of soluble protein (up to 10% total protein) were obtained after overnight induction at 25 °C. However, a 2.5-h induction at 30 °C also provided sufficient yields (5–10% total protein) for enzyme assays.

The recombinant McyI protein precipitated in the presence of 40% ammonium sulfate and eluted from the Ni²⁺-charged affinity column at an imidazole concentration of ~300 mM. The recombinant protein eluate was of >95% purity and was eluted at concentrations of 1–2.5 mg/ml (Fig. 5).

Subunit Composition of McyI—The purified McyI protein eluted from the size exclusion column at 27.8 min, corresponding to a molecular mass of 85 kDa (dimeric form) (Fig. 6). The collected elution fractions (25–30 min) displayed OAA reductase activity of ~12.5–14 μmol/min/mg, which was comparable with that of the unfractionated enzyme (data not shown).

Biochemical and Kinetic Properties of McyI—McyI was stable for >2 weeks at 4 °C without significant loss of activity and for at least 6 months at –20 °C in 15% glycerol. Plots of McyI OAA reductase activity after 1-min incubations at various temperatures were bell-shaped with an optimum of ~45 °C at pH 7. However, McyI was relatively unstable at higher temperatures (90% drop in activity following preincubation at 50 °C). The pH optimum for the McyI OAA reductase activity was 7.1 however, the enzyme maintained at least 80% of its activity between pH 6.5 and 7.5 at 25 °C (Fig. 7).

McyI displayed weak 3-MeMal, D-Mal, and L-Mal oxidase activities (~0.2–0.7 μmol/min/mg of protein under the described conditions). However, oxidation of D-2-HGA or D-3-PGA could not be detected. Because of strong product inhibition and the high concentration of enzyme required for each assay, we were unable to obtain kinetic constants for the oxidative reactions.

The reduction of OAA was the major *in vitro* activity observed for McyI, with $V_{\max}^{\text{app}} = 15.2 \mu\text{mol/min/mg}$ of protein at 37 °C (Fig. 8). However, high concentrations of substrate (>0.8 mM) inhibited the reaction. The enzyme was also able to reduce α-KG, although the rates of catalysis were much lower ($V_{\max}^{\text{app}} \sim 3.6 \mu\text{mol/min/mg}$ of protein). The OAA and α-KG reductase reactions both obeyed regular Michaelis-Menten kinetics (Table 3).

McyI was able to utilize phosphorylated and dephosphorylated dinucleotide cofactors, although the rates of catalysis for NADH were ~90% lower than those obtained for NADPH ($V_{\max}^{\text{app}} \sim 6.5 \mu\text{mol/min/mg}$ of protein) with equivalent amounts of enzyme. Detailed kinetic data could therefore not be obtained using NADH.

End Product Analysis—NMR spectroscopic analysis confirmed that malate was the product of the OAA reductase reaction (supplemental Fig. S1).

Inhibition Assays—The OAA reductase activity of McyI was inhibited by D-Mal ($I_{50} = 2.2 \text{ mM}$) and 3-MeMal ($I_{50} = 0.7 \text{ mM}$) in a negatively cooperative manner. Interestingly, L-Mal did not inhibit the reaction, nor did L-Ser, D-Asp, L-Asp, D-2-HGA, or D-3-PGA. The α-KG reductase activity of McyI was inhibited by 3-MeMal ($I_{50} = 2.3 \text{ mM}$) and D-2-HGA ($I_{50} = 20.5 \text{ mM}$) (Fig. 9 and Table 3).

DISCUSSION

To assess the role of *mcyl* in microcystin production, a variety of hepatotoxic and nontoxic strains of cyanobacteria were screened for *mcyl* orthologs. With the exception of *P. agardhii* CYA126, the degenerate primers successfully amplified an ~790-bp PCR fragment from all microcystin-producing strains tested (Table 1). Interestingly, nearly half of all the nontoxic cyanobacterial strains

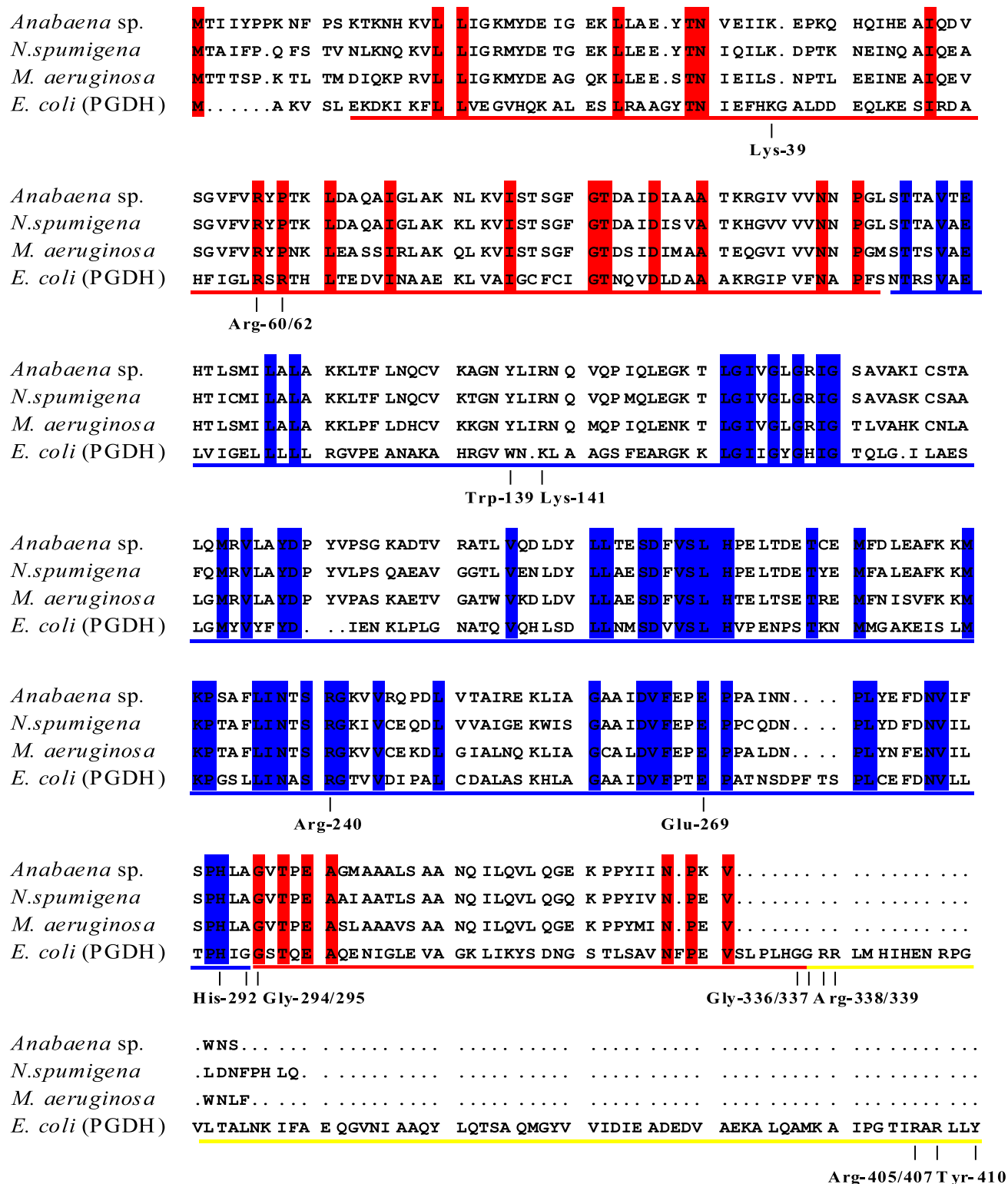


FIGURE 3. Alignment of *McyI* (*M. aeruginosa*, NCBI accession number AAF00955; and *Anabaena* sp., AA062580), *NdaH* (*N. spumigena*, AA064409), and *PGDH* (*E. coli*, P08328). Structurally important amino acid residues and the NAD-binding signature are indicated (see "Results" for details). Consensus residues are highlighted. Colored regions define the three domains of *PGDH*: the nucleotide-binding domain (residues 108–294; blue), the substrate-binding domain (residues 7–107 and 295–336; red), and the regulatory domain (residues 338–409; yellow).

examined tested positive for *mcyl*. These results reflect those of previous studies that identified *mcyl* genes in several nontoxic *Microcystis* strains (3, 19, 20). It is likely that these strains have

reverted to a nontoxic phenotype because of mutations within their *mcyl* biosynthesis genes or within *mcyl* regulatory regions. Previous studies have demonstrated that the *mcyl* gene cluster does

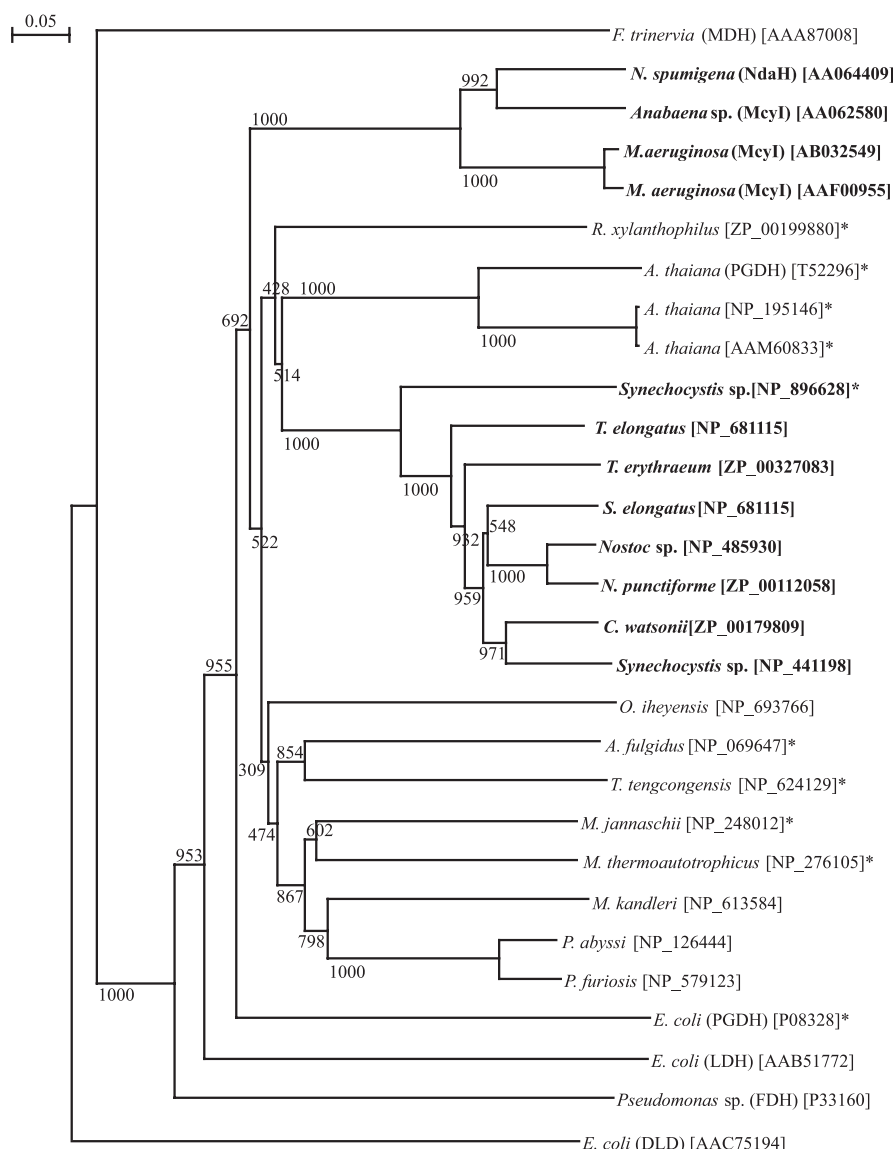


FIGURE 4. Phylogenetic tree incorporating *McyI* and similar dehydrogenases. The phylogenetic tree encompasses PGDH homologs from cyanobacteria (**boldface**) and other organisms. An *E. coli* D-lactate dehydrogenase (*DLD*) constitutes the artificial outgroup. Asterisks indicate sequences with ACT (regulatory) domains. For a detailed list of the sequences used, see Table 2. Bootstrap values derived from 1000 replicates are given. The scale at the top of the tree corresponds to 5% divergence between sequences.

It is interesting to note that *P. agardhii* CYA126 does not possess *mcylI*, yet it is still capable of producing microcystin (22). *mcylI* is therefore not critical for all types of microcystin production, but may be required for the biosynthesis of certain microcystin isoforms. The most frequently reported microcystin isoforms contain D-MeAsp at position 3, yet *P. agardhii* CYA126 produces only the less toxic [D-Asp³]microcystin variants (1). *mcylI* may therefore be specific to strains producing [D-MeAsp³]microcystin. The fact that *mcylI* has been sequenced only from strains that are capable of producing [D-MeAsp³]microcystin (*i.e.* *M. aeruginosa* and *Anabaena* sp. 90) further supports this supposition. If *mcylI* genes can be identified specifically in other *P. agardhii* strains that produce [D-MeAsp³]microcystin, a strong argument could be made in support of the involvement of *McyI* in D-MeAsp biosynthesis. It may also prove valuable to screen nodularin-producing cyanobacteria for *ndaH* homologs, as only a few different isoforms of this toxin have been reported, one of which contains D-Asp in place of D-MeAsp at position 1 (23).

Homology-based searches indicated that *McyI* is a cytosolic enzyme belonging to the 2-hydroxy-acid dehydrogenase family. Although its closest characterized relative, *A. thaliana* PGDH, is involved in Ser metabolism, sequence data suggest an alternative function for *McyI*. An immediately obvious difference

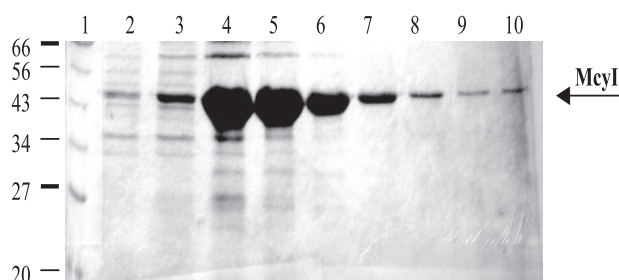


FIGURE 5. Purification of *McyI*. Hexahistidine-tagged *McyI* was eluted from a Ni²⁺-charged HiTrap column. Lane 1, broad-range molecular mass standards (shown in kilodaltons); lanes 2–10, *McyI* elution fractions 2–10.

not well tolerate mutations with respect to toxin biosynthesis; in fact, the mutation of several individual *mcyl* genes (*mcylA*, *mcylB*, *mcylD*, *mcylE*, *mcylF*, and *mcylH*) has led to the production of mutant strains with nontoxic phenotypes (3, 19, 21).

between the peptide sequence of *McyI* and those of bacterial PGDHs is its lower subunit molecular mass (37 versus 44 kDa). This is largely due to the fact that *McyI* lacks an ACT domain (residues 338–409 in *E. coli* PGDH) (24). These regulatory domains have been linked to a wide range of metabolic enzymes that are controlled by amino acids in a concentration-dependent fashion (25).

An alternative regulatory mechanism such as transcriptional control may negate the need for an ACT domain in *McyI* and other cyanobacterial enzymes (*e.g.* those present in the phylogenetic tree in Fig. 4). The fact that *McyI* has two promoters, *i.e.* its own individual promoter as well as the central *mcylD–J* promoter, strongly supports this hypothesis (26, 27).

A close comparison of the primary peptide sequence of *McyI* with those of other 2-hydroxy-acid dehydrogenases in the data bases revealed further interesting characteristics of the protein. A

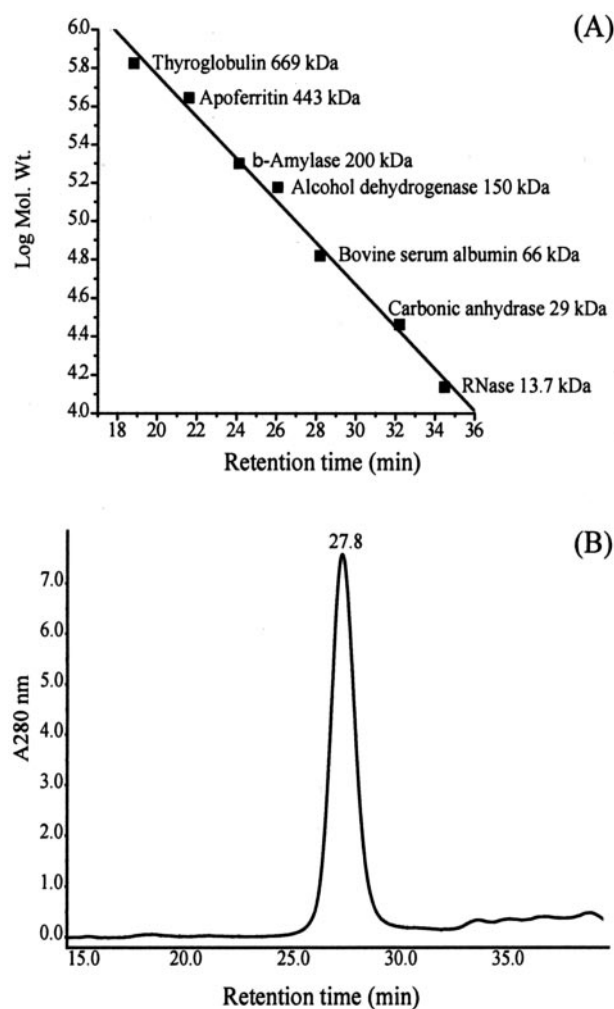


FIGURE 6. **Determination of McyI subunit organization.** A, elution standard curve for protein molecular mass standards; B, chromatogram of purified recombinant McyI. The peak at 27.8 min corresponds to the McyI dimer (85 kDa, including the His tag). All samples were run on an ÄKTA Basic 900 series fast protein liquid chromatography apparatus fitted with a Superdex 200 10/300 GL column.

large proportion of amino acids in McyI are highly conserved among most of the other dehydrogenases examined, including the NAD(P)-binding signature encompassing residues 158–186 of the McyI sequence. This nucleotide-binding domain is conserved among all 2-hydroxy-acid dehydrogenases, including PGDH, MDH, LDH, and glycerate dehydrogenase. The identification of a nucleotide-binding domain within McyI suggests that it is a NAD(P)-dependent enzyme with an oxidoreductase function similar to that of PGDH.

The cationic residues that are thought to form an electrostatic environment for the binding of the negatively charged substrate at the active site of PGDH include Lys³⁹, Arg⁶⁰, Arg⁶², Lys¹⁴¹, and Arg²⁴⁰. The results of mutating these residues in PGDH showed that Arg⁶⁰, Arg⁶², Lys¹⁴¹, and Arg²⁴⁰ play distinct roles in the binding of the substrate to the active site (28). Arg²⁴⁰ is conserved in McyI and all other sequences in the alignment. This basic residue plays an important role in anchoring the C-1 hydroxyl group of 3-PGA during catalysis. Similar basic residues are present in MDH and LDH. The additional basic residues (Arg⁶² and Lys¹⁴¹) are unique

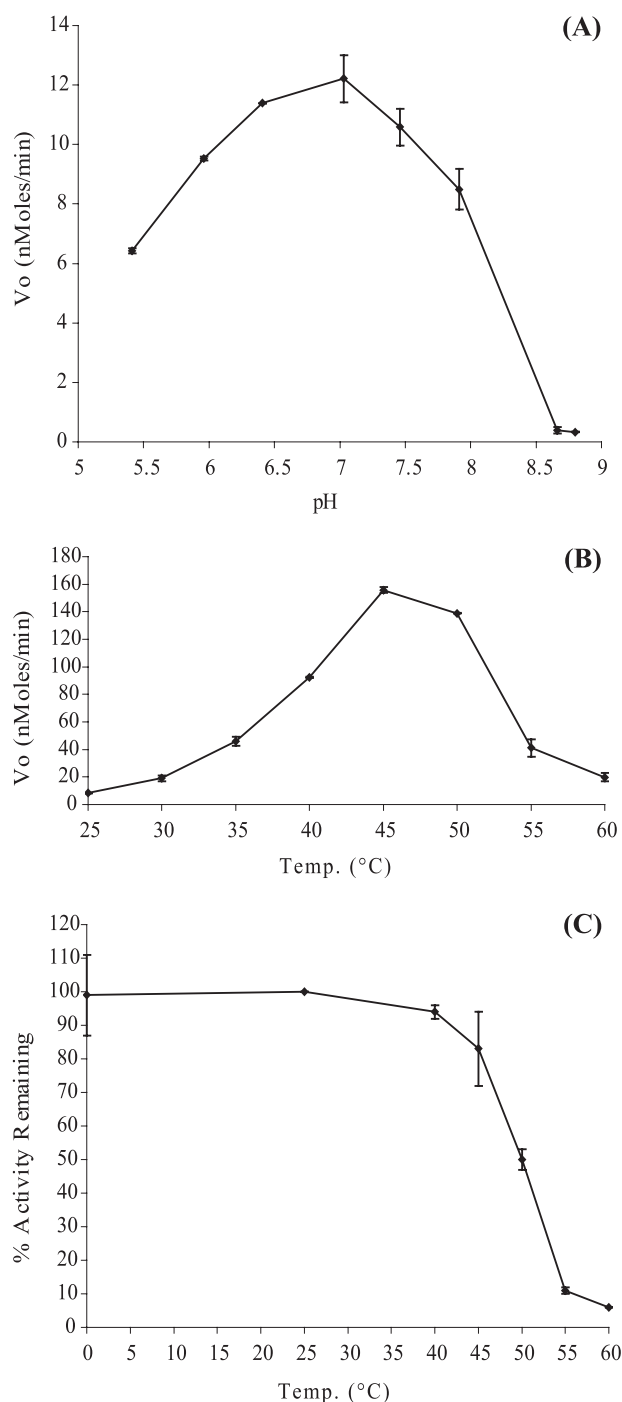


FIGURE 7. **Biochemical properties of the McyI OAA reductase activity.** A and B, OAA reductase activity of McyI at different pH values and different temperatures, respectively; C, McyI thermal stability. See "Results" for details regarding reaction conditions. The data are presented as the means of two to three separate experiments.

to PGDH and may interact with an acidic group at the distal end of the substrate (28). The fact that McyI possesses Arg²⁴⁰ but lacks Arg⁶² and Lys¹⁴¹ suggests that a 2-hydroxy acid other than 3-PGA is the substrate of this cyanobacterial enzyme.

In PGDH, Arg⁶⁰, Arg⁶², and Lys¹⁴¹ work in tandem to bind the phosphate group of the substrate (28). In the *M. aeruginosa*, *Anabaena* sp., and *N. spumigena* sequences, Arg⁶⁰ is

Characterization of Mcyl

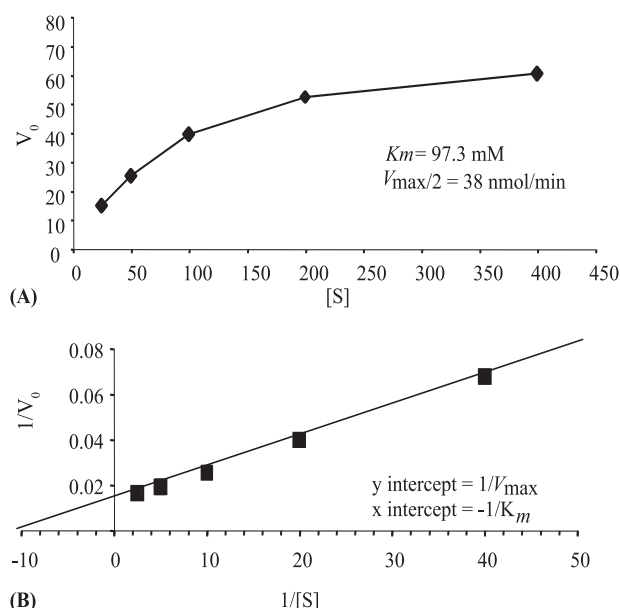


FIGURE 8. Kinetic plots for the Mcyl OAA reductase activity. A, V versus $[S]$ plot; B, Lineweaver-Burk plot. $[S]$ equals millimolar substrate (OAA). The data presented are from a single experiment using 5 μ g of purified Mcyl and 0.25 mM NADPH at pH 7 (see "Results" for details). These results were reproducible (at least four times on separate days) within an error margin of 10%.

TABLE 3
Kinetic and inhibition parameters of reactions catalyzed by Mcyl

Reaction ^a	K_m^{app} μ M	V_{max}^{app} μ mol/min/mg protein	Inhibition (I_{50}) ^b mM
OAA	97.3 ± 1.5	15.2 ± 0.2	0.7 ± 0.01 (3-MeMal), 2.2 ± 0.03 (D-Mal)
NADPH	35.8 ± 1.8	6.5 ± 0.3	Not tested
α -KG	2886.6 ± 116.2	3.6 ± 0.1	2.3 ± 0.06 (3-MeMal), 20.5 ± 0.2 (D-2-HGA)

^a Kinetic analysis of the α -KG and OAA reductase activities of Mcyl was carried out in 1-ml reactions each containing 0.25 mM NADPH, 5 μ g of purified enzyme, and various amounts of substrate in reaction buffer (pH 7). Kinetic analysis of the NADPH oxidase activity of Mcyl was performed in 1-ml reactions each containing 5 μ g of purified enzyme, 0.8 mM OAA, and various amounts of NADPH in reaction buffer (pH 7). Initial velocities were measured by monitoring the disappearance of NADPH at 340 nm for 0.5 min at 37 °C. No deviations in linearity were observed on plots of kinetic data. The data presented are from a single experiment; however, each experiment was reproduced at least four times with <10% deviation in results between trials.

^b Assays were performed in 1-ml of reaction buffer (pH 7) containing 0–8 mM inhibitor (L-Ser, 3-MeMal, L-Mal, D-Mal, L-Asp, D-Asp, D-2-HGA, or D-3-PGA), 0.25 mM NADPH, 5 μ g of enzyme, and 0.2 mM OAA or 1 mM α -KG. I_{50} is the concentration of inhibitor required for 50% inhibition in standard enzyme assays with saturating substrate. The data are presented as the means of two to three separate experiments performed consecutively.

conserved; however, Arg⁶² and Lys¹⁴¹ are not. In Mcyl and NdaH, Arg⁶² is replaced by Pro. This cyclic amino acid, which can markedly influence protein architecture, also lacks the hydrophilic charged side chain of Arg. Despite this non-conservative substitution, the secondary structures of Mcyl, NdaH, and PGDH did not appear to differ at this site, with each protein possessing a helix-loop-sheet composition. The fact that *A. thaliana* PGDH contains glycine in place of Arg⁶², as do most of the other cyanobacterial dehydrogenases, suggests that certain substitutions at this position may not be critical to activity because the *A. thaliana* PGDH can complement *E. coli* PGDH (*serA*) mutants (29). Lys¹⁴¹ is replaced by Arg in Mcyl as well as in most other sequences in the alignment. This is a conservative substitu-

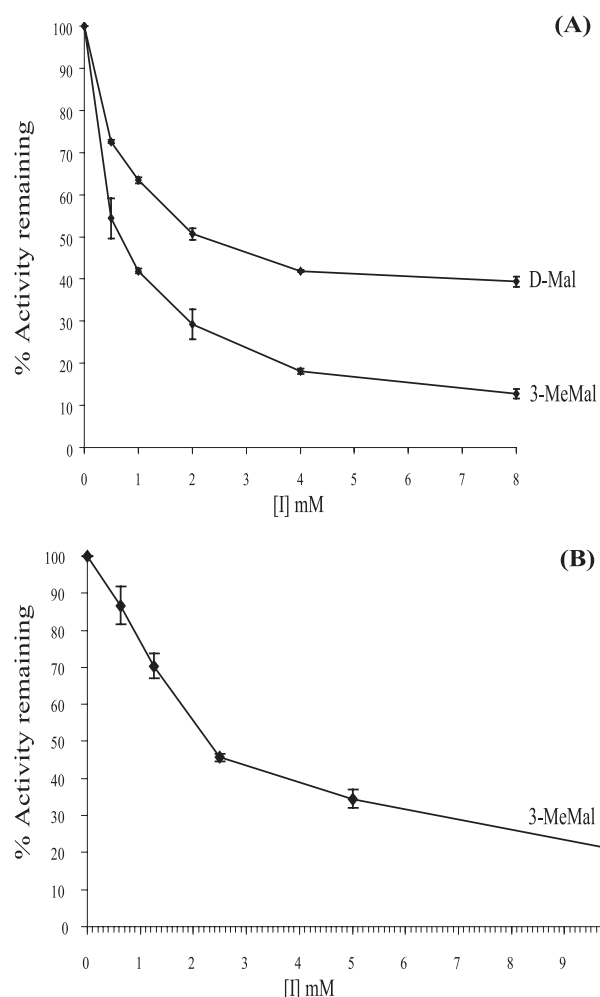


FIGURE 9. Inhibition of Mcyl reductase activities. A, inhibition of OAA reductase activity by D-Mal and 3-MeMal; B, inhibition of α -KG reductase activity by 3-MeMal. The x axes correspond to inhibitor concentration, and the y axes correspond to percentage enzyme activity remaining. One-hundred percent activity corresponds to activity in the absence of inhibitor. The data are presented as the means of two to three separate experiments.

tion (both amino acids are positively charged) and probably has little effect on the overall structure and function of the enzyme. In summary, in PGDH, Arg⁶⁰, Arg⁶², and Lys¹⁴¹ are critical for binding the phosphate group of the substrate (28). Although the overall architecture of Mcyl and NdaH may not be affected by substitutions in this region, the results suggest that these cyanobacterial enzymes preferentially bind non-phosphorylated 2-hydroxy acids.

In *E. coli* PGDH, Trp¹³⁹ participates in intersubunit contact near the active-site catalytic residues, where it fits within a hydrophobic pocket created by Pro²⁷⁰, Pro²⁹¹, and Phe²⁷⁷ (28, 30). Although the hydrophobic binding pocket is generally conserved in Mcyl, Trp¹³⁹ is replaced by tyrosine. This may have several implications for the structure and function of the enzyme. Although Trp and Tyr are both aromatic amino acids, Tyr lacks an indole ring and has a phenolic group. It has been recently demonstrated that, upon removal of the indole ring of Trp¹³⁹, PGDH dissociates into dimers (30). We therefore hypothesized that Mcyl functions as a dimer. Subsequent analysis of Mcyl by size exclusion chromatography supported this

hypothesis. As Trp¹³⁹ also plays a key role in the cooperativity of Ser binding and inhibition, we predict that Mcyl is a non-cooperative enzyme.

His²⁹² is important for catalyzing the interconversion of 3-phosphohydroxypyruvate and 3-PGA in PGDH. In addition, Glu²⁶⁹ acts in tandem with His²⁹² to form a proton shuttle, as seen in many dehydrogenases (28). The conservation of these residues within Mcyl again supports an oxidoreductase function for this enzyme.

In PGDH, Gly²⁹⁴ and Gly²⁹⁵ form the link between the substrate-binding and nucleotide-binding domains, which form the active-site cleft of the enzyme. Mutations of these residues affect the K_{cat} of the enzyme without appreciably affecting sensitivity to serine (31). Although Gly²⁹⁵ is conserved in Mcyl and NdaH, Gly²⁹⁴ is replaced by Ala. Mutational studies have shown that G294A substitutions do not affect the catalytic capacity of PGDH (31), and therefore, this conservative substitution should not influence the K_{cat} of Mcyl or NdaH. Indeed, homologous enzymes can tolerate a number of different amino acids at this position, as evidenced by the alignment (Fig. 3) in which several sequences have either Ser or Glu in the first position and Lys, Arg, or Asn in the second position.

In an attempt to understand the evolution of Mcyl in the context of other 2-hydroxy-acid dehydrogenases such as PGDH, MDH, and LDH, a phylogenetic tree was constructed encompassing sequences from plants, Archaea, and eubacteria, including several species of cyanobacteria (Fig. 4). Interestingly, the cyanobacterial sequences cluster polyphyletically. Although the subgroup B cyanobacterial proteins appear to share a common ancestor with plant PGDHs, the hepatotoxin-associated proteins form a phylogenetically distinct subgroup (subgroup A). Mcyl and NdaH must have therefore diverged early in the evolution of PGDHs, prior to the divergence of the archaeal, plant, and subgroup B cyanobacterial protein lineages.

In a similar phylogenetic study in which PGDHs from a wide range of organisms were investigated, Ali *et al.* (32) reported that sequences from the order Bacillales also display a polyphyletic distribution. They concluded that many lateral gene transfer events, together with drastic insertion/deletion events, occurred during the evolution of PGDH, making the history of this superfamily very complex. The distribution of ACT domains among 2-hydroxy-acid dehydrogenases contributes to this complexity. In the phylogenetic tree presented in Fig. 4, it appears that the ancestral PGDH possessed an ACT domain, yet this domain was lost in some (but not all) subsequent generations. It is interesting to note that even proteins from closely related organisms (*e.g.* *Synechocystis* sp. PCC6803 and *Synechocystis* sp. WH8102) may differ when it comes to possession of an ACT domain. These results suggest that alternative regulatory mechanisms such as transcriptional control must be in place for many of these enzymes.

Although none of the reference sequences (PGDH, LDH, MDH, and formate dehydrogenase) partitioned within subgroups A–C, the fact that PGDH from *A. thaliana* fell within subgroup B suggests that the subgroup B cyanobacterial sequences, and probably the archaeal sequences, also function in serine metabolism. Conversely, the distantly related subgroup A cyanobacterial proteins

(Mcyl and NdaH) are likely to have evolved functions specific to hepatotoxin biosynthesis.

To investigate the remarkable prospect that Mcyl may be a PGDH, the recombinant enzyme was assayed for 3-PGA dehydrogenase activity *in vitro*. However, despite extensive experimental variation, PGDH activity was not detected. The lack of PGDH activity also reflects the phylogenetic data presented in this study suggesting that Mcyl is evolutionarily distant to PGDH and belongs to a separate clade of enzymes, uniquely present in the hepatotoxic cyanobacteria. The comparative sequence data also support this notion and predict distinct functions for Mcyl and PGDH.

Although Mcyl is therefore clearly not involved in Ser metabolism, it is probable that *M. aeruginosa* possesses a true PGDH elsewhere in its genome. Genome sequencing projects and/or genetic screening studies should shed light on this topic in the near future.

Interestingly, Mcyl was able to utilize α -KG/OAA and Mal as substrates, but not lactate or pyruvate. As with most 2-hydroxy-acid dehydrogenases, the major *in vitro* activity observed for Mcyl was in the reductase direction, *i.e.* the reduction of OAA to Mal. Oxalacetate showed a 30-fold decrease in K_m^{app} over α -KG and a 100-fold increase in $V_{\text{max}}^{\text{app}}/K_m^{\text{app}}$. The higher catalytic efficiency of OAA is consistent with the hypothesis that the native substrate of Mcyl (3-methyl oxalacetate (3-MeOAA)) is a structural analog of OAA.

Both phosphorylated and dephosphorylated dinucleotide cofactors were utilized by Mcyl, yet NADPH was greatly preferred over NADH. It would be interesting to determine whether the putative cyanobacterial PGDHs used in this phylogenetic study are also NAD-specific. If so, it is likely that the nucleotide-binding domain of Mcyl evolved from a NAD-specific form to its current NADP-specific form.

As the reduction of OAA was the major *in vitro* activity observed for Mcyl, we predicted that the true physiological substrate of Mcyl must be a Mal/OAA analog. This led to the hypothesis that Mcyl catalyzes the conversion of 3-MeMal to 3-MeOAA, with subsequent transamination to MeAsp. To test this hypothesis, a racemic diastereomeric mixture of 3-MeMal was synthesized and tested as a substrate in an *in vitro* dehydrogenase assay. Unfortunately, the attempted synthesis of the unstable 3-MeOAA to test the reverse reaction (3-MeOAA to 3-MeMal) was not successful. Mcyl was able to oxidize 3-MeMal at a comparable rate to D- and L-Mal; however, there appeared to be strong end product inhibition, which significantly reduced the linear range of the assay (<30 s).

To understand the inhibitory effects of various substrates on the Mcyl reductase reactions, several inhibition assays were performed. Unlike PGDH, Mcyl was not allosterically regulated by Ser or by any other compound tested. This result was not surprising because Mcyl lacks an ACT regulatory domain. 3-MeMal and D-Mal inhibited Mcyl OAA reductase activity in a negatively cooperative fashion. 3-MeMal was the strongest inhibitor, with $I_{50} \sim 0.7$ mM. Interestingly, L-Mal had no inhibitory effects, suggesting that, like other 2-hydroxy-acid dehydrogenases, Mcyl preferentially binds substrates with D-conformations. It is therefore likely that the I_{50} for 3-MeMal is overestimated because the 3-MeMal compound was a racemic

diastereomeric mixture. These results support the hypothesis that McyI is a 3-MeMal/3-MeOAA oxidoreductase.

The nonproteinogenic amino acid 3-MeAsp is a common intermediate of the mesaconate pathway for (S)-glutamate fermentation in *Clostridium* spp. (33) and in members of the family Enterobacteriaceae (34). This unusual amino acid residue also occurs in the lipopeptide antibiotic friulimicin (35) and in the cyanobacterial hepatotoxins microcystin and nodularin (3, 7). In the mesaconate and friulimicin pathways, the route to MeAsp occurs via rearrangement of Glu to 3-MeAsp involving glutamate mutase. However, genome sequencing efforts have failed to identify glutamate mutase homologs in cyanobacteria. We propose that the cyanobacteria utilize an alternative glutamate mutase-independent biosynthetic pathway to 3-MeAsp, in which McyI plays a pivotal role.

Labeled precursor feeding experiments by Moore *et al.* (9) suggested that the MeAsp residues in microcystin and nodularin are produced via the rearrangement of citramalic acid, yet the authors were unable to identify the enzymes involved in this pathway. In this study, we have provided evidence that the 2-hydroxy-acid dehydrogenase McyI catalyzes the interconversion of 3-MeMal to 3-MeOAA. The final step in the MeAsp pathway, the conversion of 3-MeOAA to MeAsp, is likely to be catalyzed by a promiscuous Asp aminotransferase, as these enzymes occur in virtually all organisms, including cyanobacteria (36).

To our knowledge, McyI is the only reported example of a 3-MeMal/3-MeOAA oxidoreductase. On the basis of the data presented in this study, it appears that McyI and its homolog NdaH diverged from a PGDH ancestor to become NADP-dependent enzymes with specific roles in hepatotoxin production. Future mutagenesis experiments involving *mcyl* and *ndaH* will undoubtedly offer further insight into the role of these unique cyanobacterial enzymes.

REFERENCES

- Sivonen, K., and Jones, G. (1999) in *Toxic Cyanobacteria in Water: a Guide to Their Public Health Consequences, Monitoring and Management* (Chorus, I., and Bartram, J., eds) pp. 42–49, E&FN Spon, London
- Botes, D., Wessels, P., Kruger, H., Runnegar, M., Santikarn, S., Smith, R., Barna, J., and Williams, D. (1985) *J. Chem. Soc.* **1**, 2747–2748
- Tillett, D., Dittmann, E., Erhard, M., von Dohren, H., Borner, T., and Neilan, B. A. (2000) *Chem. Biol.* **7**, 753–764
- Smith, D. R., Doucette-Stamm, L. A., Deloughery, C., Lee, H., Dubois, J., Aldredge, T., Bashirzadeh, R., Blakely, D., Cook, R., Gilbert, K., Harrison, D., Hoang, L., Keagle, P., Lumm, W., Pothier, B., Qiu, D., Spadafora, R., Vicaire, R., Wang, Y., Wierzbowski, J., Gibson, R., Jiwani, N., Caruso, A., Bush, D., Safer, H., Patwell, D., Prabhakar, S., McDougall, S. N., Shimer, G., Goyal, A., Pietrokovski, S., Church, G., Daniels, C., Mao, J., Rice, P., Nolling, J., and Reeve, J. N. (1997) *J. Bacteriol.* **179**, 7135–7155
- Zhao, G., and Winkler, M. E. (1996) *J. Bacteriol.* **178**, 232–239
- Bell, J. K., Pease, P. J., Bell, J. E., Grant, G. A., and Banaszak, L. J. (2002) *Eur. J. Biochem.* **269**, 4176–4184
- Moffitt, M. C., and Neilan, B. A. (2004) *Appl. Environ. Microbiol.* **70**, 6353–6362
- Karakas, S., Narbad, A., Horn, N., Dodd, H., Par, A., Colquhoun, I., and Gasson, M. (1999) *Eur. J. Biochem.* **261**, 524–532
- Moore, R., Chen, J., Moore, B., and Patterson, G. (1991) *J. Am. Chem. Soc.* **113**, 5083–5084
- Tillett, D., and Neilan, B. A. (2000) *J. Phycol.* **36**, 251–258
- Campbell, H. D., Rogers, B. L., and Young, I. G. (1984) *Eur. J. Biochem.* **144**, 367–373
- Herter, S., Fuchs, G., Bacher, A., and Eisenreich, W. (2002) *J. Biol. Chem.* **277**, 20277–20283
- Baht, K. S., Dixit, K. N., and Rao, A. S. (1985) *Indian J. Chem.* **24**, 509–512
- Renaud, P., Hurzler, M., and Seebach, D. (1987) *Helv. Chim. Acta* **70**, 292–298
- Kakinuma, K., Teresawa, H., Li, H.-Y., Miyazaki, K., and Oshima, T. (1993) *Biosci. Biotechnol. Biochem.* **57**, 1916–1923
- Taguchi, H., and Ohta, T. (1991) *J. Biol. Chem.* **266**, 12588–12594
- Kochhar, S., Hunziker, P. E., Leong-Morgenthaler, P., and Hottinger, H. (1992) *Biochem. Biophys. Res. Commun.* **184**, 60–66
- Goldberg, J. D., Yoshida, T., and Brick, P. (1994) *J. Mol. Biol.* **236**, 1123–1140
- Nishizawa, T., Asayama, M., Fujii, K., Harada, K., and Shirai, M. (1999) *J. Biochem. (Tokyo)* **126**, 520–529
- Kaebnick, M., Rohrlack, T., Christoffersen, K., and Neilan, B. A. (2001) *Environ. Microbiol.* **3**, 669–679
- Dittmann, E., Neilan, B. A., Erhard, M., von Dohren, H., and Borner, T. (1997) *Mol. Microbiol.* **26**, 779–787
- Christiansen, G., Fastner, J., Erhard, M., Borner, T., and Dittmann, E. (2003) *J. Bacteriol.* **185**, 564–572
- Namikoshi, M., Sivonen, K., Evans, W. R., Carmichael, W. W., Rouhiainen, L., Luukkainen, R., and Rinehart, K. L. (1992) *Chem. Res. Toxicol.* **5**, 661–666
- Aravind, L., and Koonin, E. V. (1999) *J. Mol. Biol.* **287**, 1023–1040
- Schuller, D. J., Grant, G. A., and Banaszak, L. J. (1995) *Nat. Struct. Biol.* **2**, 69–76
- Kaebnick, M., Neilan, B. A., Borner, T., and Dittmann, E. (2000) *Appl. Environ. Microbiol.* **66**, 3387–3392
- Kaebnick, M., Dittmann, E., Borner, T., and Neilan, B. A. (2002) *Appl. Environ. Microbiol.* **68**, 449–455
- Grant, G. A., Kim, S., Xu, X., and Hu, Z. (1999) *J. Biol. Chem.* **274**, 5357–5361
- Ho, C. L., Noji, M., Saito, M., and Saito, K. (1999) *J. Biol. Chem.* **274**, 397–402
- Grant, G. A., Xu, X., and Hu, Z. (2000) *Arch. Biochem. Biophys.* **375**, 171–174
- Grant, G. A., Hu, Z., and Xu, X. (2001) *J. Biol. Chem.* **276**, 1078–1083
- Ali, V., Hashimoto, T., Shigeta, Y., and Nozaki, T. (2004) *Eur. J. Biochem.* **271**, 2670–2681
- Buckel, W. (2001) *Appl. Microbiol. Biotechnol.* **57**, 263–273
- Kato, Y., and Asano, Y. (1997) *Arch. Microbiol.* **168**, 457–463
- Heinzelmann, E., Berger, S., Puk, O., Reichenstein, B., Wohlleben, W., and Schwartz, D. (2003) *Antimicrob. Agents Chemother.* **47**, 447–457
- Kim, A. D., Baker, A. S., Dunaway-Mariano, D., Metcalf, W. W., Wanner, B. L., and Martin, B. M. (2002) *J. Bacteriol.* **184**, 4134–4140
- Moore, B. S. (1999) *Nat. Prod. Rep.* **16**, 653–674
- Herdman, M., Castenholz, R. W., Iteman, I., Waterbury, J. B., and Rippka, R. (2001) in *Bergey's Manual of Systematic Bacteriology* (Boone, D. R., Castenholz, R. W., and Garrity, G. M., eds) 2nd Ed., Vol. 1, p. 776, Springer-Verlag, New York
- Rippka, R., Deruelles, J., Waterbury, J. B., Herdman, M., and Stanier, R. Y. (1979) *J. Gen. Microbiol.* **111**, 1–61
- Sivonen, K., Namikoshi, M., Evans, W. R., Carmichael, W. W., Sun, F., Rouhiainen, L., Luukkainen, R., and Rinehart, K. L. (1992) *Appl. Environ. Microbiol.* **58**, 2495–2500
- Henning, M., Hertel, H., Wall, H., and Kohl, J. G. (1991) *Int. Rev. Ges. Hydrobiol.* **76**, 37–45
- Rippka, R., and Herdman, M. (1992) *Pasteur Culture Collection of Cyanobacterial Strains in Axenic Culture. Catalogue and Taxonomic Handbook, Vol. 1: Catalogue of Strains*, Institute Pasteur, Paris
- Jackson, A. R., McInnes, A., Falconer, I. R., and Runnegar, M. T. (1984) *Vet. Pathol.* **21**, 102–113
- Starr, R. C., and Zeikus, J. A. (1993) *J. Phycol.* **29**, 1–106
- Neilan, B. A., Jacobs, D., Del Dot, T., Blackall, L. L., Hawkins, P. R., Cox, P. T., and Goodman, A. E. (1997) *Int. J. Syst. Bacteriol.* **47**, 693–697
- Moffitt, M. C., and Neilan, B. A. (2001) *FEMS Microbiol. Lett.* **196**, 207–214

Characterization of the 2-Hydroxy-acid Dehydrogenase McyI, Encoded within the Microcystin Biosynthesis Gene Cluster of *Microcystis aeruginosa* PCC7806

Leanne A. Pearson, Kevin D. Barrow and Brett A. Neilan

J. Biol. Chem. 2007, 282:4681-4692.

doi: 10.1074/jbc.M606986200 originally published online December 1, 2006

Access the most updated version of this article at doi: [10.1074/jbc.M606986200](https://doi.org/10.1074/jbc.M606986200)

Alerts:

- [When this article is cited](#)
- [When a correction for this article is posted](#)

[Click here](#) to choose from all of JBC's e-mail alerts

Supplemental material:

<http://www.jbc.org/content/suppl/2006/12/04/M606986200.DC1>

Supplemental material:

<http://www.jbc.org/content/suppl/2006/12/06/M606986200.DC2>

This article cites 44 references, 15 of which can be accessed free at

<http://www.jbc.org/content/282/7/4681.full.html#ref-list-1>